Robotica (2018) volume 36, pp. 570–587. © Cambridge University Press 2018
doi:10.1017/S0263574717000595

A new kinetostatic model for humanoid robots using screw theory

Gustavo S. Toscano†, Henrique Simas‡, Eugênio B. Castelan† and Daniel Martins‡

†*Department of Automation and Systems Engineering (DAS), Federal University of Santa Catarina (UFSC), Florianópolis, Brazil. E-mails: gustavotoscano@gmail.com, eugenio.castelan@ufsc.br*
‡*Department of Mechanical Engineering (EMC), Federal University of Santa Catarina (UFSC), Florianópolis, Brazil. E-mails: {henrique.simas,daniel.martins}@ufsc.br*

(Accepted December 13, 2017. First published online: January 22, 2018)

SUMMARY

This study presents a new kinetostatic model for humanoid robots (HRs). Screw theory, together with Assur virtual chains and Davies' method, provides the required tools for the proposal of both the kinematic and static parts of the kinetostatic model. Our kinetostatic model is able to estimate the forces and couples generated at the axes of each joint of the robot, as well as one unknown contact condition between the robot and the environment around it. The proposed model is also very versatile and free of fixed coordinates and, therefore, it allows for an estimate of a great amount of information on the HR. Some results, obtained from computer simulation, are presented to validate the versatility of the proposed technique.

KEYWORDS: Humanoid robots; Kinetostatic model; Screw theory; Davies' method; Virtual chains

1. Introduction

A humanoid robot (HR) is a kind of robotic system composed of one floating base (FB), from which four serial chains that mimic four limbs of the human body depart. Depending on the combination of its limbs interacting with the environment, an HR can be described through several possible different kinematic structures. Said feature allows for the analysis of an HR according to a switching structure varying among serial, parallel, and hybrid kinematic chains [1].

The above-mentioned inherent switching structure has been widely adopted in the literature, regardless of the chosen methodology for HR modeling, considering that each structure describes mostly a supporting limb condition. In refs. [2, 3, 4, 5, 6, 7, 8], for instance, the HR is modeled as a linkage of multi-bodies and joints, and its supporting foot is considered grounded at the inertial reference frame. In refs. [9, 10, 11, 12, 13, 14, 15, 16, 17], a simplified model, which uses the linear inverted pendulum, is presented. Said methodology still uses a switching structure, since two linear inverted pendulum models are needed to describe a single HR.

The "multi-model" HR paradigm was changed when the FB concept was applied to HR modeling. The FB (yet not named as such) had its genesis in the aeronautic field of free-flying systems, in which a moving local reference frame was placed in the flight control system [18]. Then, in refs. [19, 20], the FB concept was developed and applied to a robotic system composed of a serial manipulator robot coupled to a spacecraft.

Sentis conceived the idea of free-floating systems and successfully applied it to HR models [21]. Said approach caused the "multi-model" paradigm in HR modeling to change, because no switching model structure was required. The use of the FB allowed HRs to be described with only one mechanism. Thus, both the position and orientation of these robots are completely defined by the FB's position and orientation, in addition to the positions of the robot's joints. The framework given in refs. [21, 22] also provides a dynamic model that considers forces and couples in contact with both the robot's feet and hands with the environment.

https://doi.org/10.1017/S0263574717000595 Published online by Cambridge University Press

The use of the FB concept to model HRs was a contribution made in refs. [21, 22] that enabled a more "human-like" modeling. In particular, the features obtained with the use of the FB in HR modeling facilitated motion planning and collaborative tasks among robot's limbs, since the model has become more systematized. As the feet in contact with the ground are not fixed onto any of its points, a more "human-like" description of the support contact conditions may be obtained.

Generally, in the works found in the literature, the contacts of the feet with the ground are defined through passive joints, which give HR models with some degree of under-actuation. The treatment given is based on specific solutions. In refs. [21, 22], for instance, the authors consider the motion of one or more links as a constrained motion in their model equations. In ref. [23], the authors also drew attention to the under-actuation issue observed in ref. [22] and proposed a solution based on Jacobian matrices and conditional solutions. Therefore, both approaches address the under-actuation issue by proposing conditional solutions, which lead to some loss of generality, as also observed in refs. [24, 25].

Indeed, HRs are a type of structure-varying kinematic chains whose "multi-limb" kinematic chain provides many possible interactions. That is, each posture and set of contacts with the environment is described through a different mechanism. Furthermore, the static interactions between HRs and the manipulation of different objects may also increase the number of different mechanisms through which a single HR can be described. Therefore, the development of closed-form solutions for modeling these robots is a challenge. In most works found in the literature, such as refs. [26, 27, 28, 29], the structure-varying kinematic chains feature of said robots is addressed as optimization problems with particular solutions, because each mechanism variation may have its own specific kinematic topology and, most likely, its own degree of mobility.

Based on these grounds, the main objective of this work is to present the kinetostatic model – based on screw theory [30, 31] and its tools, such as Davies' method and Assur's virtual chains [32, 31, 33, 34, 35] – for HRs, which, as a new paradigm for modeling these robots, solve the issues and propose advancement based on other modeling techniques that have already been discussed. The kinetostatic model is a combination of both kinematic and static models. The proposal also uses the advantages of the FB for modeling an HR as a free-floating system. This approach is particularly useful for robotic systems composed of one link with 6-DoF (degree of freedom) of motion in the spatial space, in which four serial kinematic chains are coupled. This framework's kinematic model has already been addressed in ref. [36], which should be consulted for further details. Therefore, this paper will focus on the static part of our kinetostatic model.

Concepts from graph theory applied to mechanism analysis [32, 31] are used to represent the HR mechanism as a single parallel mechanism. Furthermore, with respect to static scenarios and quasi-static motion, the proposed approach is not only capable of computing the required joints' torque, but also the joints' internal static actions due to constrained motions and one unknown contact condition required to achieve static equilibrium. To the best of our knowledge, there is no other result in the literature for kinetostatic modeling of HRs that shares the same features of our proposal: a single kinematic model and a single static model versatile enough to describe HRs in any given posture and to yield the amount of information that the proposed model is able to provide.

This work is organized as follows. In Section 2, the major concepts of screw theory are briefly discussed. In Section 3, the methodology to build the kinetostatic model for HRs is explained. In Section 4, some simulation results are presented to show the data the kinetostatic model is capable of estimating. Then, Section 5 presents a final discussion on the proposal.

2. Fundamental Tools

The kinetostatic model for HRs proposed in this study is based on screw theory, Assur's virtual chains, Davies' method, and graph theory, whose main concepts and techniques have already been discussed in refs. [31, 33, 34, 35].

First formulated by Mozzy [37] and systematized by Sir Robert Ball [30], screw theory can be used to analyze both spatial kinematics and statics of mechanisms. Screw theory is able to represent both the instantaneous motion of rigid bodies through the twist $\$^M = [\boldsymbol{\omega}^T \;\; \boldsymbol{v}_p^T]^T \in \mathbb{R}^6$ (see Fig. 1(a)) and the forces acting on them through the wrench $\$^A = [\boldsymbol{M}_p^T \;\; \boldsymbol{F}^T]^T$ (see Fig. 1(b)). Fundamental theorems as Poinsot's [38] and Chasles' [39] are on the basis of screw theory.

https://doi.org/10.1017/S0263574717000595 Published online by Cambridge University Press

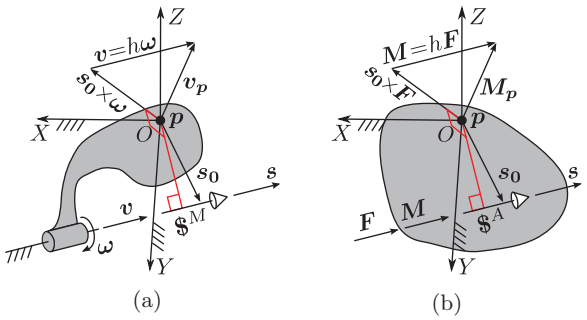


Fig. 1. The screw notation and its components. (a) The twist $\$^M$. (b) The wrench $\$^A$.

3. Kinetostatic Model of Humanoid Robots

The human body's topological structure can be split into five independent segments – head, upper-limbs (two arms), and lower-limbs (two legs) – attached to the torso –, whose motions are independent from one another. If the robot's head and neck are not considered, an HR can be seen as four independent serial chains attached to its torso and working together in order to perform any task.

3.1. Kinematic Model

The kinematic model of HRs that uses screw theory has already been proposed in ref. [36], and it is briefly addressed here in a more systematized way.

In order to apply Davies' method through screw theory, it is necessary to analyze the humanoid mechanism in its digraph representation. Fig. 2 depicts the relation between serial chains of the digraph representation of an HR and the human body. The float base link represents the robot's waist, which is the robot's local reference frame for the limbs.

Considering the robot can "touch" the world with its hands and feet, there are four ways through which the robot can make contact with the environment. According to the analysis of the mechanism and kinematics theories, each grounded contact, or a combination of them, produces different mechanisms with different kinematic topologies. Considering n_L the number of limbs of an HR and that the robot can interact with the environment through a combination of its $n_L = 4$ limbs, a single HR can generate $2^{n_L} - 1 = 15$ different mechanisms depending on how it interacts with the environment.

The main characteristic of the presented method for kinematic modeling of HRs is that all of the 15 kinematic model variations can be summarized in a single representation depicted in Fig. 3(b). Our proposal is that through the use of virtual chains, HRs can always be kinematically modeled as a parallel mechanism whose differential kinematics can be systematically solved with the application of Davies' method. Therefore, the objective of using Davies' method to solve differential kinematic models is to determine a suitable $\dot{\boldsymbol{q}}_{\boldsymbol{p}}$ that makes $\boldsymbol{N}_{\boldsymbol{s}}$ square and invertible in the following equation [40, 33, 34]:

$$\boldsymbol{N}\,\dot{\boldsymbol{q}} = \boldsymbol{0} \Rightarrow \begin{bmatrix} \boldsymbol{N}_s & \boldsymbol{N}_p \end{bmatrix} \begin{bmatrix} \dot{\boldsymbol{q}}_s \\ \dot{\boldsymbol{q}}_p \end{bmatrix} = \boldsymbol{0} \Rightarrow \dot{\boldsymbol{q}}_s = -\boldsymbol{N}_s^{-1}\boldsymbol{N}_p\dot{\boldsymbol{q}}_p, \tag{1}$$

in which $\boldsymbol{N}$ is the network matrix, $\dot{\boldsymbol{q}}$ is the vector of the magnitudes of the joints velocities, $\boldsymbol{N}_{\boldsymbol{p}}$, and $\boldsymbol{N}_{\boldsymbol{s}}$ are the subnetwork matrices, and $\dot{\boldsymbol{q}}_{\boldsymbol{p}}$ and $\dot{\boldsymbol{q}}_{\boldsymbol{s}}$ are, respectively, the primary and secondary vectors of magnitudes of the joints velocities [41]. Moreover, $\dot{\boldsymbol{q}}_{\boldsymbol{s}}$ is the magnitude vector of the angular velocities of the joints of the robot.

Figure 3 depicts the digraph representations of the structure of a humanoid – RL_i, LL_i, RA_i, and LA_i stands for right and left legs and arms. Fig. 3(a) depicts the digraph representation of the HR's chains plus the chain of the FB. The resulting mechanism is composed of $n_k = 51$ links , $j_k = 54$ joints, and $c = 4$ circuits (see Fig. 3(b)), and $\lambda = 6$ is the dimension of its operational space. Thus, in Eq. (1), $\boldsymbol{N} \in \mathbb{R}^{24\times54}$, $\dot{\boldsymbol{q}} \in \mathbb{R}^{54}$, $\boldsymbol{N}_{\boldsymbol{s}} \in \mathbb{R}^{24\times24}$, and $\boldsymbol{q}_{\boldsymbol{s}} \in \mathbb{R}^{24}$.

Therefore, to solve the differential kinematics of HRs through Davies' method, $j_k - c\lambda = 30$ primary joints velocities, the form and the vector $\dot{\boldsymbol{q}}_{\boldsymbol{p}} \in \mathbb{R}^{30}$ are needed. Since one of the purposes of

https://doi.org/10.1017/S0263574717000595 Published online by Cambridge University Press

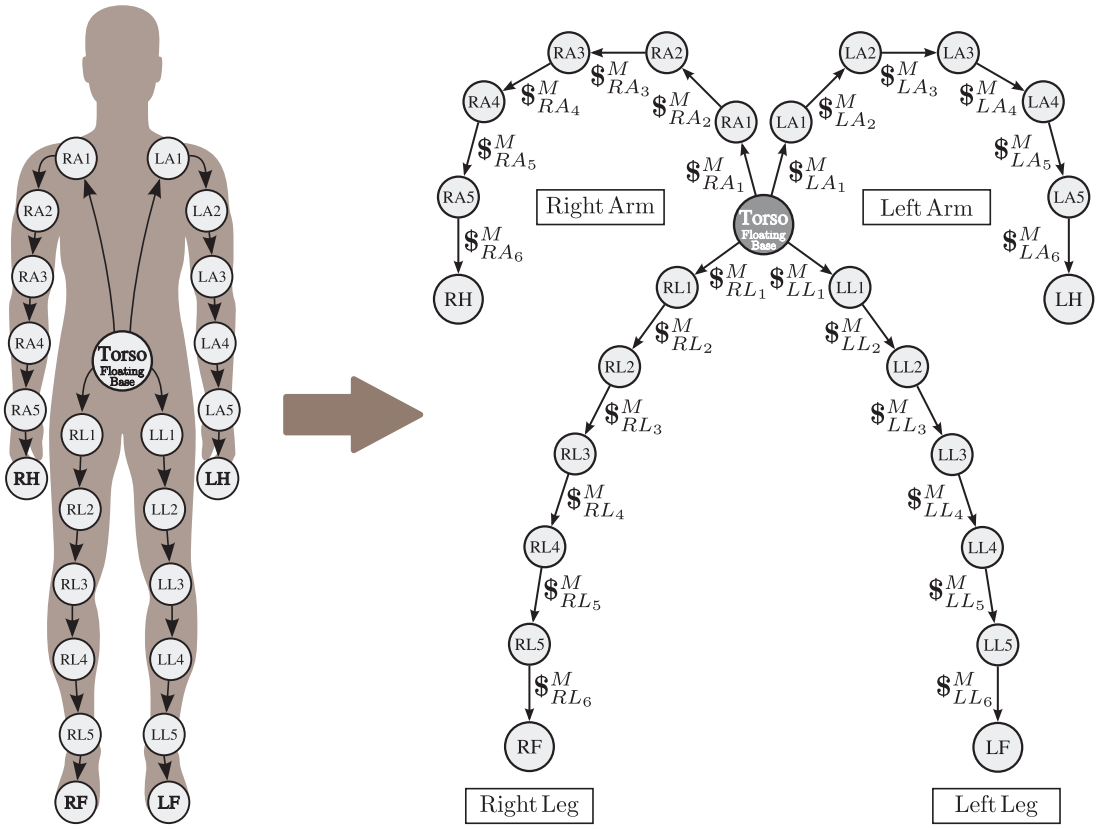


Fig. 2. The human body and its digraph representation depicting the serial chains of the digraph and its counterparts in the human body.

using virtual chains is to control the motion of "actual" chains, the vector of primary magnitudes $\dot{\boldsymbol{q}}_{\boldsymbol{p}}$ is composed of the virtual chains' joints velocities [33, 34]. As in Eq. (1), the matrices $\boldsymbol{N}_s$ and $\boldsymbol{N}_{\boldsymbol{p}}$ have fixed forms, and the key point is how to determine the vector $\dot{\boldsymbol{q}}_{\boldsymbol{p}}$.

Through the use of screw theory, the Jacobian matrix of any serial chain can be assembled with the horizontal concatenation of the normalized twists of the joints of the considered chain [32, 42]. In this paper, all virtual chains are of $P_xP_yP_zR_zR_yR_x$ type: P and R for prismatic and rotational joints, respectively, and x, y, and z are the axes of motion. Thus, the differential kinematics of this virtual chain is given by

$$\dot{\boldsymbol{X}}_{ef}^{0} = \begin{bmatrix} \boldsymbol{\omega}_{ef}^{0} \\ \boldsymbol{v}_{\boldsymbol{p}_{ef}}^{0} \end{bmatrix} = \begin{bmatrix} \hat{\$}_{px}^{M} & \hat{\$}_{py}^{M} & \hat{\$}_{pz}^{M} & \hat{\$}_{rz}^{M} & \hat{\$}_{ry}^{M} & \hat{\$}_{rx}^{M} \end{bmatrix} \begin{bmatrix} \dot{q}_{v_{px}} \\ \dot{q}_{v_{py}} \\ \dot{q}_{v_{pz}} \\ \dot{q}_{v_{rz}} \\ \dot{q}_{v_{ry}} \\ \dot{q}_{v_{rx}} \end{bmatrix} = \boldsymbol{J}_{vc}\left(\boldsymbol{q}_v\right)\dot{\boldsymbol{q}}_v, \tag{2}$$

in which the vector $\boldsymbol{X}_{ef}^{0} \in \mathbb{R}^6$ describes the position and orientation of the end-effector of the virtual chain in relation to the inertial referential frame, $\boldsymbol{\omega}_{ef}^{0} \in \mathbb{R}^3$ and $\boldsymbol{v}_{\boldsymbol{p}_{ef}}^{0} \in \mathbb{R}^3$ are, respectively, the angular and linear velocities vectors of the end-effector relative to the inertial reference frame. The p and r indexes of the normalized twists $\hat{\$}^M$ are related to prismatic and rotational joints, respectively. $\boldsymbol{J}_{vc} \in \mathbb{R}^{6\times6}$ is the screw Jacobian matrix of the virtual chain (vc) and $\boldsymbol{q}_v \in \mathbb{R}^6$ is the vector of the joints' angular position of the chain.

https://doi.org/10.1017/S0263574717000595 Published online by Cambridge University Press

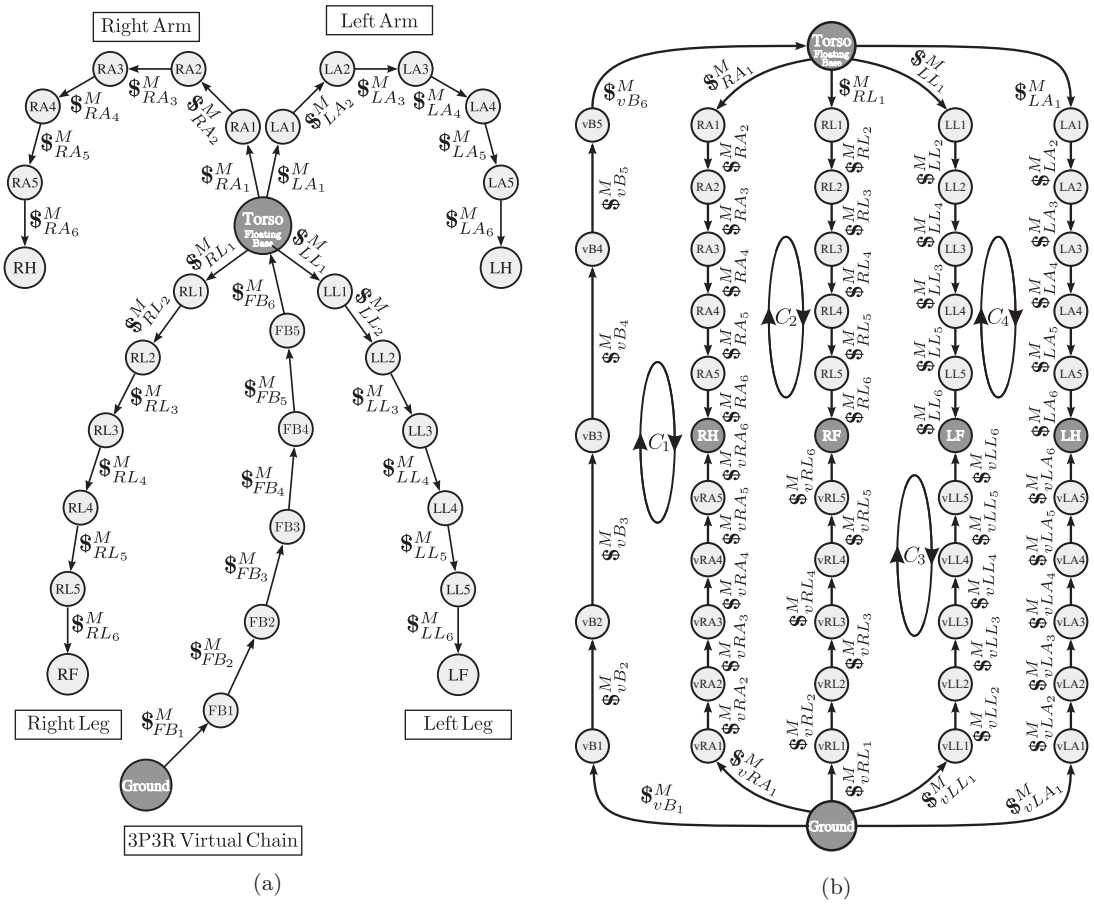


Fig. 3. Digraph representation of HRs models. (a) Serial representation. (b) Parallel representation.

By noting that Fig. 3(b) is a general kinematic representation of any HR with a rigid torso with 6-DoF per limb plus five virtual chains, which amounts to four circuits, and six DoF per virtual chain, the following properties can be verified as true:

Property 1. The velocities of the primary joints $\dot{\boldsymbol{q}}_{\boldsymbol{p}}$ of Eq. (1), according to Fig. 3(b), are computed as follows:

$$\underbrace{\begin{bmatrix} \dot{\boldsymbol{X}}_B^0 \\ \dot{\boldsymbol{X}}_{RF}^0 \\ \dot{\boldsymbol{X}}_{LF}^0 \\ \dot{\boldsymbol{X}}_{RH}^0 \\ \dot{\boldsymbol{X}}_{LH}^0 \end{bmatrix}}_{\dot{\boldsymbol{X}}^0} = \underbrace{\begin{bmatrix} \boldsymbol{J}_{vc}\left(\boldsymbol{q}_{v_B}\right) & \bar{\boldsymbol{0}} & \bar{\boldsymbol{0}} & \bar{\boldsymbol{0}} & \bar{\boldsymbol{0}} \\ \bar{\boldsymbol{0}} & \boldsymbol{J}_{vc}\left(\boldsymbol{q}_{v_{RL}}\right) & \bar{\boldsymbol{0}} & \bar{\boldsymbol{0}} & \bar{\boldsymbol{0}} \\ \bar{\boldsymbol{0}} & \bar{\boldsymbol{0}} & \boldsymbol{J}_{vc}\left(\boldsymbol{q}_{v_{LL}}\right) & \bar{\boldsymbol{0}} & \bar{\boldsymbol{0}} \\ \bar{\boldsymbol{0}} & \bar{\boldsymbol{0}} & \bar{\boldsymbol{0}} & \boldsymbol{J}_{vc}\left(\boldsymbol{q}_{v_{RA}}\right) & \bar{\boldsymbol{0}} \\ \bar{\boldsymbol{0}} & \bar{\boldsymbol{0}} & \bar{\boldsymbol{0}} & \bar{\boldsymbol{0}} & \boldsymbol{J}_{vc}\left(\boldsymbol{q}_{v_{LA}}\right) \end{bmatrix}}_{\mathbb{J}\left(\boldsymbol{q}_p\right)} \underbrace{\begin{bmatrix} \dot{\boldsymbol{q}}_{v_B} \\ \dot{\boldsymbol{q}}_{v_{RL}} \\ \dot{\boldsymbol{q}}_{v_{LL}} \\ \dot{\boldsymbol{q}}_{v_{RA}} \\ \dot{\boldsymbol{q}}_{v_{LA}} \end{bmatrix}}_{\dot{\boldsymbol{q}}_p}, \tag{3}$$

where $\bar{\boldsymbol{0}} \in \mathbb{R}^{6\times 6}$ null matrix and $\dot{\boldsymbol{X}}^0$ is defined by the trajectories generated for the FB – waist –, feet, and hands of the robot.

Property 2. Setting $\boldsymbol{q}_{\boldsymbol{s}} = [\boldsymbol{q}_{RL}^T \ \boldsymbol{q}_{LL}^T \ \boldsymbol{q}_{RA}^T \ \boldsymbol{q}_{LA}^T]^T$ and by Fig. 3(b), the subnetwork matrices $\boldsymbol{N}_{\boldsymbol{p}}$ and $\boldsymbol{N}_{\boldsymbol{s}}$ are built as follows:

https://doi.org/10.1017/S0263574717000595 Published online by Cambridge University Press

$$N_p = \begin{bmatrix} \boldsymbol{J}_{vc}\left(\boldsymbol{q}_{v_B}\right) & \bar{\mathbf{0}} & \bar{\mathbf{0}} & -\boldsymbol{J}_{vc}\left(\boldsymbol{q}_{v_{RA}}\right) & \bar{\mathbf{0}} \\ \bar{\mathbf{0}} & -\boldsymbol{J}_{vc}\left(\boldsymbol{q}_{v_{RL}}\right) & \bar{\mathbf{0}} & \boldsymbol{J}_{vc}\left(\boldsymbol{q}_{v_{RA}}\right) & \bar{\mathbf{0}} \\ \bar{\mathbf{0}} & \boldsymbol{J}_{vc}\left(\boldsymbol{q}_{v_{RL}}\right) & -\boldsymbol{J}_{vc}\left(\boldsymbol{q}_{v_{LL}}\right) & \bar{\mathbf{0}} & \bar{\mathbf{0}} \\ \bar{\mathbf{0}} & \bar{\mathbf{0}} & \boldsymbol{J}_{vc}\left(\boldsymbol{q}_{v_{LL}}\right) & \bar{\mathbf{0}} & -\boldsymbol{J}_{vc}\left(\boldsymbol{q}_{v_{LA}}\right) \end{bmatrix} \tag{4}$$

and

$$N_s = \begin{bmatrix} \bar{\mathbf{0}} & \bar{\mathbf{0}} & \boldsymbol{J}_{RA}^{B,0}\left(\boldsymbol{q}_{RA}\right) & \bar{\mathbf{0}} \\ \boldsymbol{J}_{RL}^{B,0}\left(\boldsymbol{q}_{RL}\right) & \bar{\mathbf{0}} & -\boldsymbol{J}_{RA}^{B,0}\left(\boldsymbol{q}_{RA}\right) & \bar{\mathbf{0}} \\ -\boldsymbol{J}_{RL}^{B,0}\left(\boldsymbol{q}_{RL}\right) & \boldsymbol{J}_{LL}^{B,0}\left(\boldsymbol{q}_{LL}\right) & \bar{\mathbf{0}} & \bar{\mathbf{0}} \\ \bar{\mathbf{0}} & -\boldsymbol{J}_{LL}^{B,0}\left(\boldsymbol{q}_{LL}\right) & \bar{\mathbf{0}} & \boldsymbol{J}_{LA}^{B,0}\left(\boldsymbol{q}_{LA}\right) \end{bmatrix}, \tag{5}$$

in which $\boldsymbol{J}_{RL}^{B,0}\left(\boldsymbol{q}_{RL}\right)$, $\boldsymbol{J}_{LL}^{B,0}\left(\boldsymbol{q}_{LL}\right)$, $\boldsymbol{J}_{RA}^{B,0}\left(\boldsymbol{q}_{RA}\right)$, and $\boldsymbol{J}_{LA}^{B,0}\left(\boldsymbol{q}_{LA}\right)$ are the screw Jacobian matrices of the "actual" chains from the FB of the robot, given in the coordinates of the inertial reference frame.

3.2. Static Model

For the static analysis of both robots and mechanisms using the framework of Davies' method, the external forces acting on the robot have to be internalized, which will result in a superconstrained chain [40]. The static analysis using Davies' method can be extended to fixed base mechanisms with serial chains by closing the mechanism at its contact with the environment, which is made by its end-effector, using one virtual chain [43].

Recalling the property of our model in which Fig. 3(b) covers all 15 mechanisms generated by a single HR, this feature also has its counterpart related to our static model, but with a different interpretation. Now, the 15 possible kinematic models generated from a single HR model can be summarized in a single static model (Fig. 4) with four variations. Our proposal is that, using a suitable choice of input and output vectors, our static model can be systematically solved with Davies' method using screw theory. The objective of our static model using Davies' method framework, for instance, is to determine a suitable input vector $\boldsymbol{\Psi_p}$ that makes $\hat{\boldsymbol{A}}_{\boldsymbol{NS}}$ square and invertible in the static equilibrium system's equations:

$$\hat{\boldsymbol{A}}_{\boldsymbol{N}}\,\boldsymbol{\Psi} = \mathbf{0} \Rightarrow \begin{bmatrix} \hat{\boldsymbol{A}}_{\boldsymbol{NS}} & \hat{\boldsymbol{A}}_{\boldsymbol{NP}} \end{bmatrix} \begin{bmatrix} \boldsymbol{\Psi_S} \\ \boldsymbol{\Psi_P} \end{bmatrix} = \mathbf{0} \Rightarrow \boldsymbol{\Psi_S} = -\hat{\boldsymbol{A}}_{\boldsymbol{NS}}^{-1}\hat{\boldsymbol{A}}_{\boldsymbol{NP}}\boldsymbol{\Psi_P}, \tag{6}$$

where $\hat{\boldsymbol{A}}_{\boldsymbol{NS}}$ is the secondary subnetwork of unit actions' matrix, $\hat{\boldsymbol{A}}_{\boldsymbol{NP}}$ is the primary subnetwork of unit actions' matrix, $\boldsymbol{\Psi_S}$ is the secondary wrenches' magnitude vector, and $\boldsymbol{\Psi_P}$ is the primary wrenches' magnitude vector [41].

A robot can passively interact with the environment around it by means of forces eventually applied to its links. The HR structure addressed in this study contains 13 links subjected to action forces, which are applied to them, and to four possibilities of contact – active interaction – with the environment. One may choose the inputs and outputs of the static model as follows: the inputs are the set of forces that can eventually be applied to each one of the 13 links plus the gravitational force of the center of mass (CoM) of each link. The outputs, in addition to the internal actions of each joint (forces and couples in the x, y, and z axes), one among the four possible contacts may be chosen to be the unknown contact conditions.

Figure 4 depicts the basic digraph representation for static modelling of HRs. The subindex j refers to the static relation between two links made by the joint between them. In addition, the arrows labeled by the subindex l refers to the external static action exerted on a link (arrows that depart from the real links of the robot and arrive at the ground link). The wrench that represents the external acting forces

https://doi.org/10.1017/S0263574717000595 Published online by Cambridge University Press

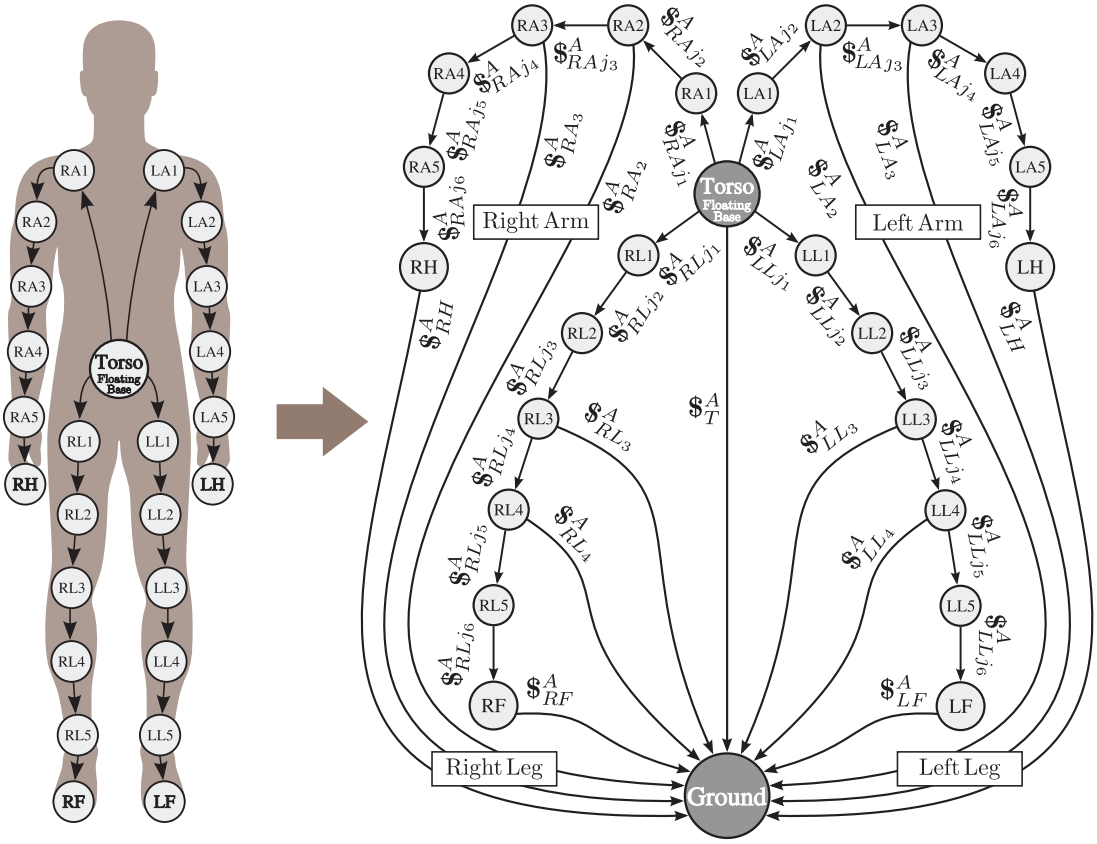


Fig. 4. Digraph representation of our static model for humanoid robots.

applied to the real links is given by the following:

$$\$_l^A = \$_{l_{CoM}}^A + \sum_{i=1}^{ext\,f} \$_{l_{Fi}}^A = \hat{\$}_l^A \psi_l, \tag{7}$$

in which $\$_{l_{CoM}}^A$ is the wrench of the gravitational force of the CoM of the link l, $ext\,f$ is the number of all external forces applied to the same link, $\$_{l_{Fi}}^A$ is the wrench of the force $\boldsymbol{F}_i$ applied to the link l, $\hat{\$}_l^A$ is its normalized wrench, and ψ_l is the magnitude of the normalized wrench $\hat{\$}_l^A$.

The wrench representation of a joint has to account for the concepts of both mobility and constraint of the joints [44]. The sum of both the mobility and constraints of a kinematic pair must be equal to λ: for a rotational joint with workspace being $\mathbb{R}^3$ has both 1 mobility and 5 constraints. Therefore, using the sum of unit wrench representation, the static action in that kinematic pair is [40]

$$\$_j^A = \hat{\$}_{j_{Fx}}^A \psi_{j_{Fx}} + \hat{\$}_{j_{Fy}}^A \psi_{j_{Fy}} + \hat{\$}_{j_{Fz}}^A \psi_{j_{Fz}} + \hat{\$}_{j_{Mx}}^A \psi_{j_{Mx}} + \hat{\$}_{j_{My}}^A \psi_{j_{My}} + \hat{\$}_{j_{Mz}}^A \psi_{j_{Mz}},$$

in which the mobility can transmit force/couple at the moving axis of the joint, and the others are the forces/couples at the axes made by the constrained motion [44]. Likewise, the unknown contact conditions can also be represented by the sum of their unit normalized wrenches multiplied by their respective magnitudes as follows:

$$\begin{aligned}\$_{Cont}^A = {} & \hat{\$}_{Cont_{Fx}}^A \psi_{Cont_{Fx}} + \hat{\$}_{Cont_{Fy}}^A \psi_{Cont_{Fy}} + \hat{\$}_{Cont_{Fz}}^A \psi_{Cont_{Fz}} + \dots \\ & \cdots + \hat{\$}_{Cont_{Mx}}^A \psi_{Cont_{Mx}} + \hat{\$}_{Cont_{My}}^A \psi_{Cont_{My}} + \hat{\$}_{Cont_{Mz}}^A \psi_{Cont_{Mz}}.\end{aligned}$$

https://doi.org/10.1017/S0263574717000595 Published online by Cambridge University Press

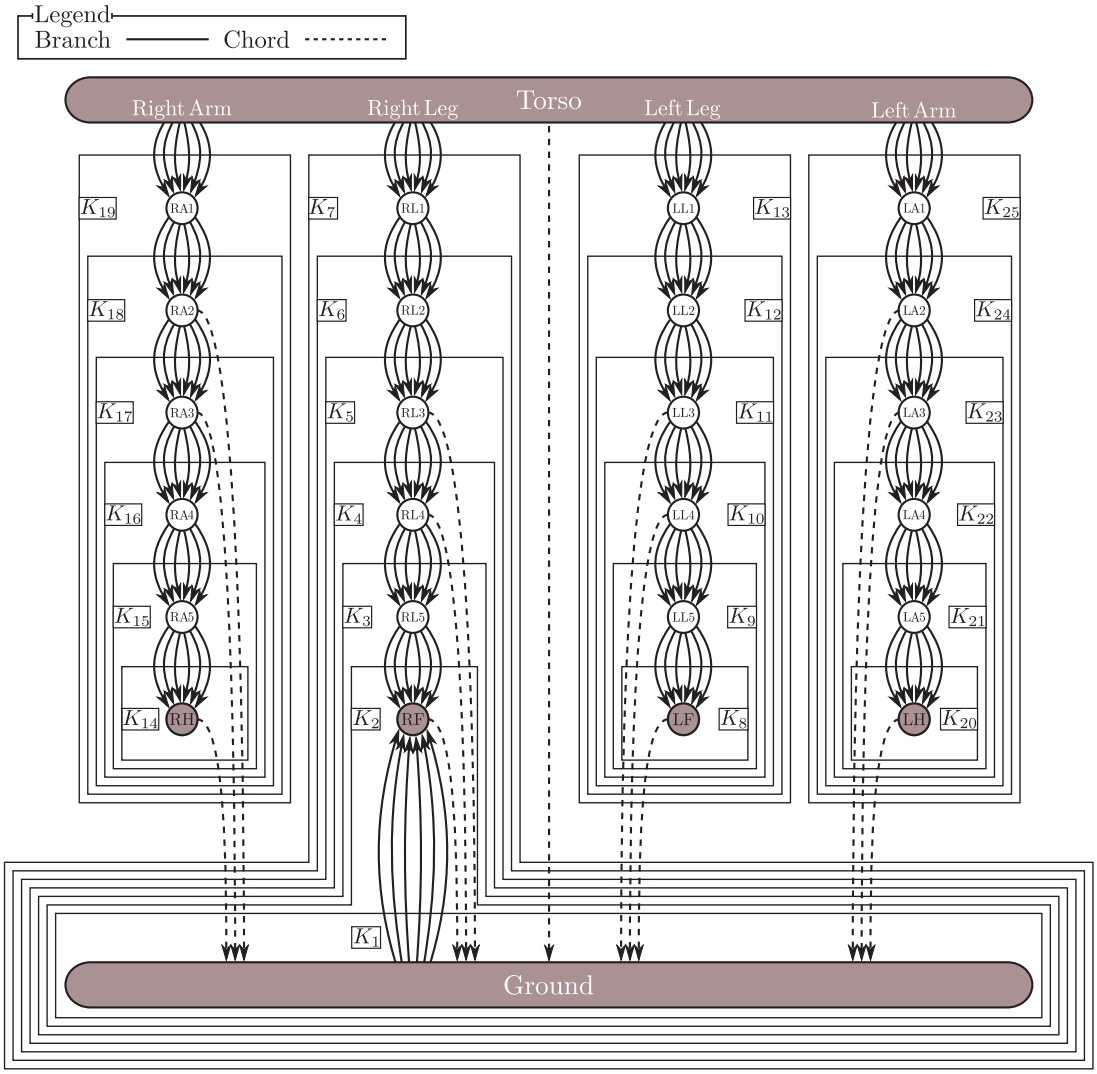


Fig. 5. Action digraph of an HR considering the contact between the right foot and the ground as the unknown contact condition. It also depicts the fundamental cutsets of the considered spanning-tree graph [40, 45].

Considering the concepts discussed herein, the arrows in Fig. 4 represent the static actions of the system. The structural analysis of mechanisms, provided by screw theory and its tool, allows for the proposal of one generic static model for HRs. In all situations, the static model of HRs is built with the use of the structure in Fig. 4 and the proposed model describes the interaction between the links of the HR and the environment.

For instance, when the supporting leg is the right one and the static contact conditions are placed between the right foot and the ground, the fundamental cutsets [40, 45], which generate the equations of the system, are defined by Fig. 5. Figure 5 is a more specific representation of an HR – derived from Fig. 4 – when the unknown contact conditions are placed between the right foot and the ground.

By definition, a robot with n_s links has $K = n_s - 1$ fundamental cutsets [40, 45]. Each fundamental cutset K_i is related to one constraint relation to static equilibrium conditions. Although the unknown contact conditions can be arbitrarily chosen – which generates different cutsets in Fig. 5 – in this paper, the contact between the right foot of the robot and the ground is considered to be the unknown contact conditions (Fig. 4).

Based on Fig. 5, it is possible to verify that, according to the spanning-tree graph of the system, humanoid robotic systems are composed of four serial chains and $n_s = 26$ links in which the latter generates $K = 25$ fundamental cutsets. Thus, the settings of the systems are: $\lambda = 6$ workspace dimension; $j_s = 24$ joints; $a_{ext} = 13$ external static actions at the links; $C_{Cont} = 6$ unknown contact

https://doi.org/10.1017/S0263574717000595 Published online by Cambridge University Press

conditions, which are here considered the contact conditions between the right foot and the ground. Then, the number of static variables of the system is given by

$$C = \lambda j_s + a_{ext} + C_{Cont} \Rightarrow C = 163. \tag{8}$$

Then, according to Eq. (8) and $K = 25$ fundamental cutsets, the network of the unit action matrix $\hat{\boldsymbol{A}}_{\boldsymbol{N}}$ has dimension 150×163 and the vector of wrenches' magnitude $\boldsymbol{\Psi} \in \mathbb{R}^{163}$.

The objective is to calculate the static variables of the joints and the contact conditions between the right foot and the ground, as shown in Fig. 5. Thus, it is possible to calculate $\boldsymbol{\Psi_S} \in \mathbb{R}^{C-a_{ext}}$ with a suitable choice of $\boldsymbol{\Psi_P} \in \mathbb{R}^{a_{ext}}$, because $\hat{\boldsymbol{A}}_{\boldsymbol{NS}} \in \mathbb{R}^{\lambda K \times \lambda K}$ ($\lambda K = (C - a_{ext}) = 150$) is invertible.

Based on Fig. 5, the fundamental cutsets K_i, for $i = 1, \ldots, 7$, will be placed at the chain whose contact condition with the environment one wishes to calculate. Furthermore, although the proposed method has four variations – each one related to an unknown contact condition –, these variations can be built through minor changes to the model to include the particularities of each variation, because the values of j_s, K, a_{ext}, C_{Cont}, and the number of static variables per joint are all fixed.

In order to assemble the network of unit actions matrix $\hat{\boldsymbol{A}}_{\boldsymbol{N}}$, two more matrices have to be built: the unit action cutset matrix $\hat{\boldsymbol{A}}_{\boldsymbol{D}} \in \mathbb{R}^{\lambda \times C}$ and the fundamental cutset matrix $\boldsymbol{Q_A} \in \mathbb{R}^{K \times C}$ [40, 33, 34]. In order to assemble the matrix $\hat{\boldsymbol{A}}_{\boldsymbol{D}}$, the vector of the wrenches' magnitudes $\boldsymbol{\Psi} = \left[\boldsymbol{\Psi}_{\boldsymbol{S}}^T \;\; \boldsymbol{\Psi}_{\boldsymbol{P}}^T\right]^T \in \mathbb{R}^C$ have to be assembled first, as follows.

The inputs of the system are given by the vector $\boldsymbol{\Psi_P} \in \mathbb{R}^{a_{ext}}$, which is composed of 13 magnitudes of the wrenches of the external forces acting on the 13 links of the humanoid structure, given by

$$\boldsymbol{\Psi_P} = \begin{bmatrix} \psi_{Torso} & \psi_{RL1} & \psi_{RL2} & \psi_{RL3} & \psi_{LL1} & \psi_{LL2} & \psi_{LL3} & \cdots \\ \cdots & \psi_{RA1} & \psi_{RA2} & \psi_{RA3} & \psi_{LA1} & \psi_{LA2} & \psi_{LA3} \end{bmatrix}^T,$$

in which *RL*, *LL*, *RA*, and *LA* stand for right and left legs, and right and left arms. The index 1, 2, and 3 of the legs are related to the thigh, shin, and foot of each leg. The index 1, 2, and 3 of the arms are related to the upper-arm, forearm, and hand of each arm.

The output of the system is given based on the vector $\boldsymbol{\Psi_S} \in \mathbb{R}^{C-a_{ext}}$, which is composed of internal static actions on the axes of each one of the joints, plus the unknown contact static conditions to be placed at only one contact between the robot and the environment. At first, one must consider that each one of the joints generates its own unknown magnitude vector, given by

$$\boldsymbol{\Psi}_{Ji} = \begin{bmatrix} \psi_{Ji_{Fx}} & \psi_{Ji_{Fy}} & \psi_{Ji_{Fz}} & \psi_{Ji_{Mx}} & \psi_{Ji_{My}} & \psi_{Ji_{Mz}} \end{bmatrix}^T,$$

in which $i = 1, \ldots, j_s$ joints. The unknown contact static conditions also insert into the system the unknown magnitude vector, given by

$$\boldsymbol{\Psi}_{Cont} = \begin{bmatrix} \psi_{Cont_{Fx}} & \psi_{Cont_{Fy}} & \psi_{Cont_{Fz}} & \psi_{Cont_{Mx}} & \psi_{Cont_{My}} & \psi_{Cont_{Mz}} \end{bmatrix}^T.$$

Therefore, the $\boldsymbol{\Psi_S}$ is assembled through the vertical concatenation of $\boldsymbol{\Psi}_{Ji}$, for $i = 1, \ldots, j_s$, and $\boldsymbol{\Psi}_{Cont}$, as follows:

$$\boldsymbol{\Psi_S} = \begin{bmatrix} \boldsymbol{\Psi}_{J1}^T & \boldsymbol{\Psi}_{J2}^T & \cdots & \boldsymbol{\Psi}_{Jj_s}^T & \boldsymbol{\Psi}_{Cont}^T \end{bmatrix}^T.$$

Given any HR with a rigid torso, 6-DoF per limb, with the following parameters j_s, K, a_{ext}, and fixed number of static variables, the following property for assembling the matrix $\hat{\boldsymbol{A}}_{\boldsymbol{D}}$ holds true:

Property 3. The unit action cutset matrix $\hat{\boldsymbol{A}}_{\boldsymbol{D}}$ can be partitioned into 3 submatrices according to the order of the magnitudes in the vector $\boldsymbol{\Psi}$, as follows:

$$\hat{\boldsymbol{A}}_{\boldsymbol{D}} = \begin{bmatrix} \hat{\boldsymbol{A}}_{\boldsymbol{D}_{Joints}} & \hat{\boldsymbol{A}}_{\boldsymbol{D}_{Fcont}} & \hat{\boldsymbol{A}}_{\boldsymbol{D}_{Fext}} \end{bmatrix}$$

https://doi.org/10.1017/S0263574717000595 Published online by Cambridge University Press

in which

$$\hat{\boldsymbol{A}}_{\boldsymbol{D}_{Joints}} = \left[\hat{\$}^A_{1_{Fx}}\hat{\$}^A_{1_{Fy}}\hat{\$}^A_{1_{Fz}}\hat{\$}^A_{1_{Mx}}\hat{\$}^A_{1_{My}}\hat{\$}^A_{1_{Mz}}\hat{\$}^A_{2_{Fx}}\hat{\$}^A_{2_{Fy}}\ldots\ldots\hat{\$}^A_{j_{s_{Fx}}}\hat{\$}^A_{j_{s_{Fy}}}\hat{\$}^A_{j_{s_{Fz}}}\hat{\$}^A_{j_{s_{Mx}}}\hat{\$}^A_{j_{s_{My}}}\hat{\$}^A_{j_{s_{Mz}}}\right] \in \mathbb{R}^{\lambda\times\lambda j_s},$$

$$\hat{\boldsymbol{A}}_{\boldsymbol{D}_{Fcont}} = \left[\hat{\$}^A_{Cont_{F_x}}\hat{\$}^A_{Cont_{F_y}}\hat{\$}^A_{Cont_{F_z}}\hat{\$}^A_{Cont_{M_x}}\hat{\$}^A_{Cont_{M_y}}\hat{\$}^A_{Cont_{M_z}}\right] \in \mathbb{R}^{\lambda\times C_{Cont}}$$

and

$$\hat{\boldsymbol{A}}_{\boldsymbol{D}_{Fext}} = \left[\hat{\$}^A_{Torso}\hat{\$}^A_{RL_1}\hat{\$}^A_{RL_2}\hat{\$}^A_{RL_3}\hat{\$}^A_{LL_1}\hat{\$}^A_{LL_2}\hat{\$}^A_{LL_3}\hat{\$}^A_{RA_1}\hat{\$}^A_{RA_2}\hat{\$}^A_{RA_3}\hat{\$}^A_{LA_1}\hat{\$}^A_{LA_2}\hat{\$}^A_{LA_2}\right] \in \mathbb{R}^{\lambda\times a_{ext}}.$$

The matrix $\hat{\boldsymbol{A}}_{\boldsymbol{D}_{Joints}}$ is the portion of $\hat{\boldsymbol{A}}_{\boldsymbol{D}}$ relative to the wrenches of the joints of the robot, whose normalized wrenches depend only on the joints variables; $\hat{\boldsymbol{A}}_{\boldsymbol{D}_{Fcont}}$ is the portion of $\hat{\boldsymbol{A}}_{\boldsymbol{D}}$ relative to the wrenches of the unknown static contact conditions, whose normalized wrenches depend on the position of the considered contact point; and $\hat{\boldsymbol{A}}_{\boldsymbol{D}_{Fext}}$ is the portion of $\hat{\boldsymbol{A}}_{\boldsymbol{D}}$ concerning the wrenches of the external forces acting on the links of the robot.

In order to apply Davies' method to compute the magnitude of the wrenches of the static model using Eq. (6), the fundamental cutset matrix has to be assembled first in order to build the unit actions matrix $\hat{\boldsymbol{A}}_{\boldsymbol{N}}$. Henceforth, the term $\boldsymbol{0}_{k\times i}$ stands for a null matrix whose dimension is $k \times i$, and the term $\boldsymbol{1}_{k\times i}$ stands for a matrix of ones whose dimension is $k \times i$. The fundamental cutset matrix $\boldsymbol{Q}_{\boldsymbol{A}}$, built through using the action digraph depicted in Fig. 5, can be partitioned as follows:

$$\boldsymbol{Q}_{\boldsymbol{A}_{25\times 163}} = \begin{bmatrix} \boldsymbol{0}_{1\times 144} & \boldsymbol{1}_{1\times 6} & -1 & -\boldsymbol{1}_{1\times 12} \\ \mathcal{J}_{24\times 144} & \boldsymbol{0}_{24\times 6} & \mathcal{K}_{24\times 1} & \mathcal{C}_{24\times 12} \end{bmatrix}, \quad \text{for } \mathcal{K} = \begin{bmatrix} \boldsymbol{1}_{6\times 1} \\ \boldsymbol{0}_{18\times 1} \end{bmatrix}. \tag{9}$$

Figure 5 shows that each limb generates six fundamental cutsets, which should be organized according to the order of the magnitudes in the vector $\boldsymbol{\Psi}$.

The proposed model enables the allocation of one contact with unknown static conditions in only one of the robot's limbs, which generates four variations of the static model: each one related to the link whose static contact conditions with the environment is unknown.

Given any HR whose static model can be represented in Fig. 4, composed of a rigid torso link, with 6 DoF per limb, 13 links on which 13 external forces act, with C static variables and the order of the magnitudes of the wrenches in the vector of magnitudes $\boldsymbol{\Psi}$, the following property holds true. But, before that, the matrix $\mathcal{I} \in \mathbb{R}^{6\times 36}$ is defined as

$$\mathcal{I} = \begin{bmatrix} 0 & 0 & 0 & 0 & 0 & 1 \\ 0 & 0 & 0 & 0 & 1 & 0 \\ 0 & 0 & 0 & 1 & 0 & 0 \\ 0 & 0 & 1 & 0 & 0 & 0 \\ 0 & 1 & 0 & 0 & 0 & 0 \\ 1 & 0 & 0 & 0 & 0 & 0 \end{bmatrix} \otimes \boldsymbol{1}_6$$

in order to ease the notation, and four more matrices are defined as follows:

$$\mathcal{L} = \begin{bmatrix} 0 & 0 & -1 \\ 0 & 0 & -1 \\ 0 & -1 & -1 \\ -1 & -1 & -1 \\ -1 & -1 & -1 \\ -1 & -1 & -1 \end{bmatrix}, \mathcal{L}_{\boldsymbol{c}} = \begin{bmatrix} 1 & 1 & 0 \\ 1 & 1 & 0 \\ 1 & 0 & 0 \\ 0 & 0 & 0 \\ 0 & 0 & 0 \\ 0 & 0 & 0 \end{bmatrix}, \mathcal{A} = \begin{bmatrix} 0 & 0 & -1 \\ 0 & 0 & -1 \\ 0 & 0 & -1 \\ 0 & -1 & -1 \\ -1 & -1 & -1 \\ -1 & -1 & -1 \end{bmatrix} \text{ and } \mathcal{A}_{\boldsymbol{c}} = \begin{bmatrix} 1 & 1 & 0 \\ 1 & 1 & 0 \\ 1 & 1 & 0 \\ 1 & 0 & 0 \\ 0 & 0 & 0 \\ 0 & 0 & 0 \end{bmatrix}.$$

https://doi.org/10.1017/S0263574717000595 Published online by Cambridge University Press

Property 4. Given any posture of a HR, and depending on where the unknown contact conditions is placed, the submatrices $\mathcal{J}$ and $\mathcal{C}$ of the fundamental cutsets matrix $\boldsymbol{Q_A}$ can assume the values according to the following:

- Right foot

$$\mathcal{J} = \begin{bmatrix} \mathcal{I} & \mathbf{0}_{6\times36} & \mathbf{0}_{6\times36} & \mathbf{0}_{6\times36} \\ \mathbf{0}_{6\times36} & \mathcal{I} & \mathbf{0}_{6\times36} & \mathbf{0}_{6\times36} \\ \mathbf{0}_{6\times36} & \mathbf{0}_{6\times36} & \mathcal{I} & \mathbf{0}_{6\times36} \\ \mathbf{0}_{6\times36} & \mathbf{0}_{6\times36} & \mathbf{0}_{6\times36} & \mathcal{I} \end{bmatrix}, \quad \mathcal{C} = \begin{bmatrix} \mathcal{L}_c & \mathbf{1}_{6\times3} & \mathbf{1}_{6\times3} & \mathbf{1}_{6\times3} \\ \mathbf{0}_{6\times3} & \mathcal{L} & \mathbf{0}_{6\times3} & \mathbf{0}_{6\times3} \\ \mathbf{0}_{6\times3} & \mathbf{0}_{6\times3} & \mathcal{A} & \mathbf{0}_{6\times3} \\ \mathbf{0}_{6\times3} & \mathbf{0}_{6\times3} & \mathbf{0}_{6\times3} & \mathcal{A} \end{bmatrix}$$

- Left foot

$$\mathcal{J} = \begin{bmatrix} \mathbf{0}_{6\times36} & \mathcal{I} & \mathbf{0}_{6\times36} & \mathbf{0}_{6\times36} \\ \mathcal{I} & \mathbf{0}_{6\times36} & \mathbf{0}_{6\times36} & \mathbf{0}_{6\times36} \\ \mathbf{0}_{6\times36} & \mathbf{0}_{6\times36} & \mathcal{I} & \mathbf{0}_{6\times36} \\ \mathbf{0}_{6\times36} & \mathbf{0}_{6\times36} & \mathbf{0}_{6\times36} & \mathcal{I} \end{bmatrix}, \quad \mathcal{C} = \begin{bmatrix} \mathbf{1}_{6\times3} & \mathcal{L}_c & \mathbf{1}_{6\times3} & \mathbf{1}_{6\times3} \\ \mathcal{L} & \mathbf{0}_{6\times3} & \mathbf{0}_{6\times3} & \mathbf{0}_{6\times3} \\ \mathbf{0}_{6\times3} & \mathbf{0}_{6\times3} & \mathcal{A} & \mathbf{0}_{6\times3} \\ \mathbf{0}_{6\times3} & \mathbf{0}_{6\times3} & \mathbf{0}_{6\times3} & \mathcal{A} \end{bmatrix}$$

- Right hand

$$\mathcal{J} = \begin{bmatrix} \mathbf{0}_{6\times36} & \mathbf{0}_{6\times36} & \mathcal{I} & \mathbf{0}_{6\times36} \\ \mathcal{I} & \mathbf{0}_{6\times36} & \mathbf{0}_{6\times36} & \mathbf{0}_{6\times36} \\ \mathbf{0}_{6\times36} & \mathcal{I} & \mathbf{0}_{6\times36} & \mathbf{0}_{6\times36} \\ \mathbf{0}_{6\times36} & \mathbf{0}_{6\times36} & \mathbf{0}_{6\times36} & \mathcal{I} \end{bmatrix}, \quad \mathcal{C} = \begin{bmatrix} \mathbf{1}_{6\times3} & \mathbf{1}_{6\times3} & \mathcal{A}_c & \mathbf{1}_{6\times3} \\ \mathcal{L} & \mathbf{0}_{6\times3} & \mathbf{0}_{6\times3} & \mathbf{0}_{6\times3} \\ \mathbf{0}_{6\times3} & \mathcal{L} & \mathbf{0}_{6\times3} & \mathbf{0}_{6\times3} \\ \mathbf{0}_{6\times3} & \mathbf{0}_{6\times3} & \mathbf{0}_{6\times3} & \mathcal{A} \end{bmatrix}$$

- Left Hand

$$\mathcal{J} = \begin{bmatrix} \mathbf{0}_{6\times36} & \mathbf{0}_{6\times36} & \mathbf{0}_{6\times36} & \mathcal{I} \\ \mathcal{I} & \mathbf{0}_{6\times36} & \mathbf{0}_{6\times36} & \mathbf{0}_{6\times36} \\ \mathbf{0}_{6\times36} & \mathcal{I} & \mathbf{0}_{6\times36} & \mathbf{0}_{6\times36} \\ \mathbf{0}_{6\times36} & \mathbf{0}_{6\times36} & \mathcal{I} & \mathbf{0}_{6\times36} \end{bmatrix}, \quad \mathcal{C} = \begin{bmatrix} \mathbf{1}_{6\times3} & \mathbf{1}_{6\times3} & \mathbf{1}_{6\times3} & \mathcal{A}_c \\ \mathcal{L} & \mathbf{0}_{6\times3} & \mathbf{0}_{6\times3} & \mathbf{0}_{6\times3} \\ \mathbf{0}_{6\times3} & \mathcal{L} & \mathbf{0}_{6\times3} & \mathbf{0}_{6\times3} \\ \mathbf{0}_{6\times3} & \mathbf{0}_{6\times3} & \mathcal{A} & \mathbf{0}_{6\times3} \end{bmatrix}$$

According to the proposed static model for HRs, it is not possible only to compute the torques at the joints of the robot as well as the chosen unknown contact conditions, but also to account for the perturbation forces and the contact of the other limbs with the environment at the model level. Moreover, through minor modifications, the proposed static model can be applied to HRs in order to analyze what is required by a set of known information regardless of the posture of the robot.

3.3. Computation of the kinetostatic model of humanoid robots

This section establishes an algorithm to compute the kinetostatic model of HRs. The input data is considered to be generated by any trajectory generation method and all the known forces that act on the links of the robot. Given the right set of input data, the computation of the Kinetostatic Model for HRs can be conducted with the Algorithm 1.

https://doi.org/10.1017/S0263574717000595 Published online by Cambridge University Press

Algorithm 1: Algorithm of the Kinetostatic Model for HRs

Initialization
T: total time of the simulation
ΔT: integration step
$N = length\,(0 : \Delta T : T)$
Offline Trajectory Generation
$\left[\bar{\boldsymbol{T}}^0, \dot{\boldsymbol{X}}^0, \bar{\$}^A_{Fext}\right] = \text{AnyTrajectoryGenerationMethod}\,(T, \Delta T, N)$
Inputs for the model
$\bar{\boldsymbol{T}}^0 \in \mathbb{R}^{20\times 4N}$
$\dot{\boldsymbol{X}}^0 \in \mathbb{R}^{5\lambda\times N}$
$\bar{\$}^A_{Fext} \in \mathbb{R}^{13\lambda\times N}$
Model computation
for $i = 1 \ldots N$ **do**
  Positioning Kinematics
    $\boldsymbol{q}_{\boldsymbol{s}_i} = InvKinRobotLimbs\left(\bar{\boldsymbol{T}}_i^0\right)$
    $\boldsymbol{q}_{\boldsymbol{p}_i} = InvKinVirtualChains\left(\bar{\boldsymbol{T}}_i^0\right)$
  Kinematic counterpart of the Kinetostatic Model
    $\dot{\boldsymbol{q}}_{\boldsymbol{p}_i} = InvDiffKinVirtualChains(\dot{\boldsymbol{X}}_i^0)$ using Property 1
    $\dot{\boldsymbol{q}}_{\boldsymbol{s}_i} = InvDiffKinRobotJoints(\dot{\boldsymbol{q}}_{\boldsymbol{p}_i})$ with $\boldsymbol{N_p}$ and $\boldsymbol{N_s}$ given by Property 2
  Static counterpart of the Kinetostatic Model
    Assemble $\hat{\boldsymbol{A}}_{\boldsymbol{D}}$ using Property 3
    Define $\boldsymbol{\Psi}_{\boldsymbol{P}_i}$
    Select the matrix $\boldsymbol{Q_A}$ using Eq. (9) and the Property 4
    Assemble the matrix $\hat{\boldsymbol{A}}_{\boldsymbol{N}}$
    Compute $\boldsymbol{\Psi}_{\boldsymbol{S}_i}$ by Eq. (6)
end
Output
$\boldsymbol{q_s} \in \mathbb{R}^{24\times N}$
$\dot{\boldsymbol{q}}_{\boldsymbol{s}} \in \mathbb{R}^{24\times N}$
$\boldsymbol{\Psi_S} \in \mathbb{R}^{150\times N}$

4. Numerical Results

Some simulations were designed and performed in order to validate the proposed kinetostatic model of HRs. In the present study, for instance, the motion to be executed by the HR was to move its waist downwards and upwards, while the ground projection of the robot's center of mass (GCoM) was kept within the support polygon made on the contact surface between the right foot and the ground. Figure 6 depicts both the initial and final postures of the HR considered in the simulations.

The robot was set in a way so that its hands maintained constant position and orientation relative to its waist, and also that its left foot was kept lifted with constant position and orientation relative to the inertial reference frame. It was also set so that the waist was displaced laterally to the right side to maintain the GCoM within the support polygon, thus ensuring the static stability [46] of the robot while performing the *quasi*-static motion.

In order to perform the presented simulation, the matrix $\boldsymbol{Q_A}$ had to be assembled according to Eq. (9) and Property 4.

Henceforth, the label of each joint in its respective chain is numbered as follows: the first joint of one chain is the joint located nearest to the torso. Thus, the sixth joint (last joint) of each chain is the joint connected to the end-effector of the considered chain.

Figure 7 depicts the angular velocities of the joints of both legs that, together with the angular velocities of the joints of both arms, were estimated through the computation of the kinematic model of our kinetostatic model. The kinematic model is able to systematically solve the inverse differential

https://doi.org/10.1017/S0263574717000595 Published online by Cambridge University Press

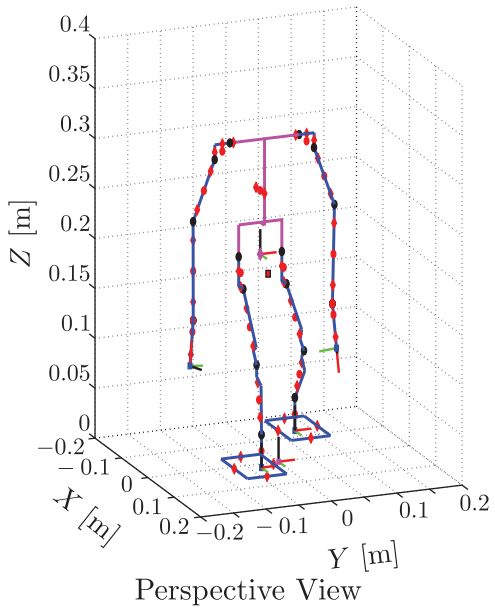


Fig. 6. Initial and final positions of the humanoid robot considered in the simulation.

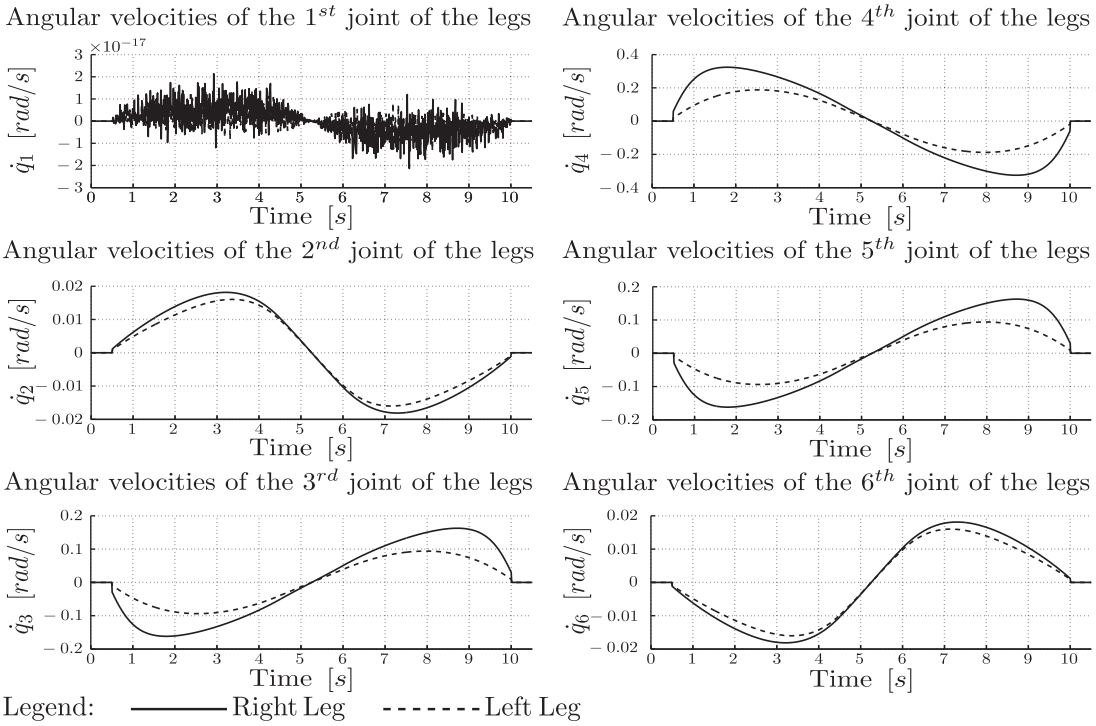


Fig. 7. Angular velocity of the joints of the right and left legs.

kinematics of HRs at once, regardless of their posture, the motion required to be performed, or the interaction between the robot and the environment around it.

The resulting data from the static simulation using the static model of our kinetostatic model focuses on the major effort of the supporting leg and the contact conditions between both the right foot and the ground. For the current simulation data, we did not consider perturbation forces at the robot's links. However, the weights of the links were considered: the inclusion of perturbation forces in the model were set to be done through adding any set of perturbation forces to the gravitational

https://doi.org/10.1017/S0263574717000595 Published online by Cambridge University Press

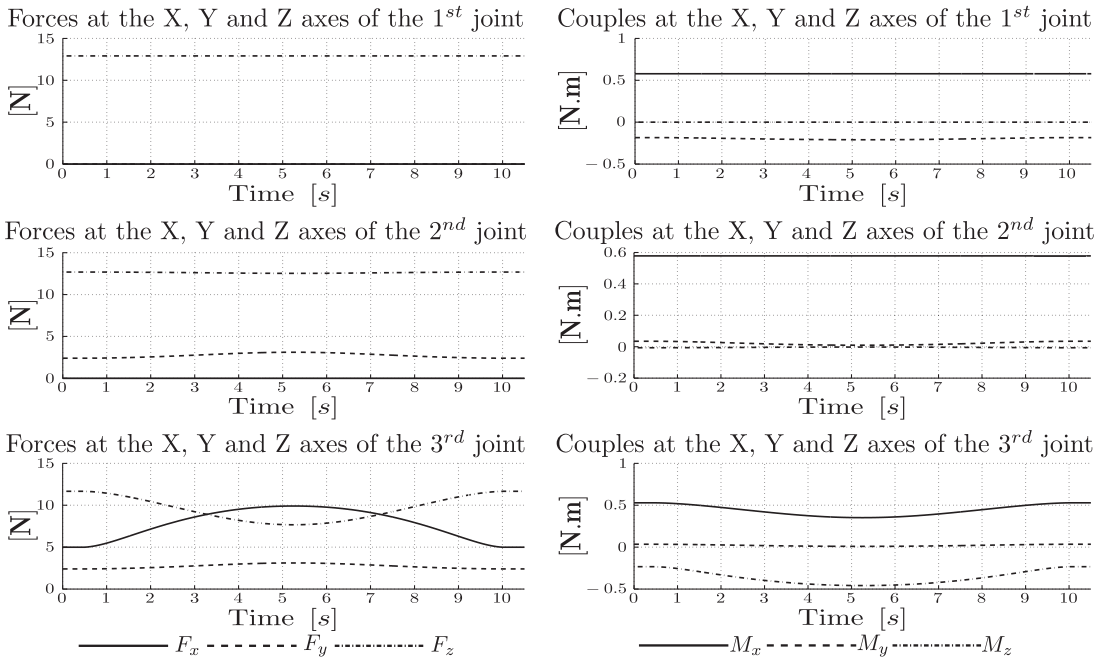


Fig. 8. Static action at the axes of the first three joints of the right leg during the simulation.

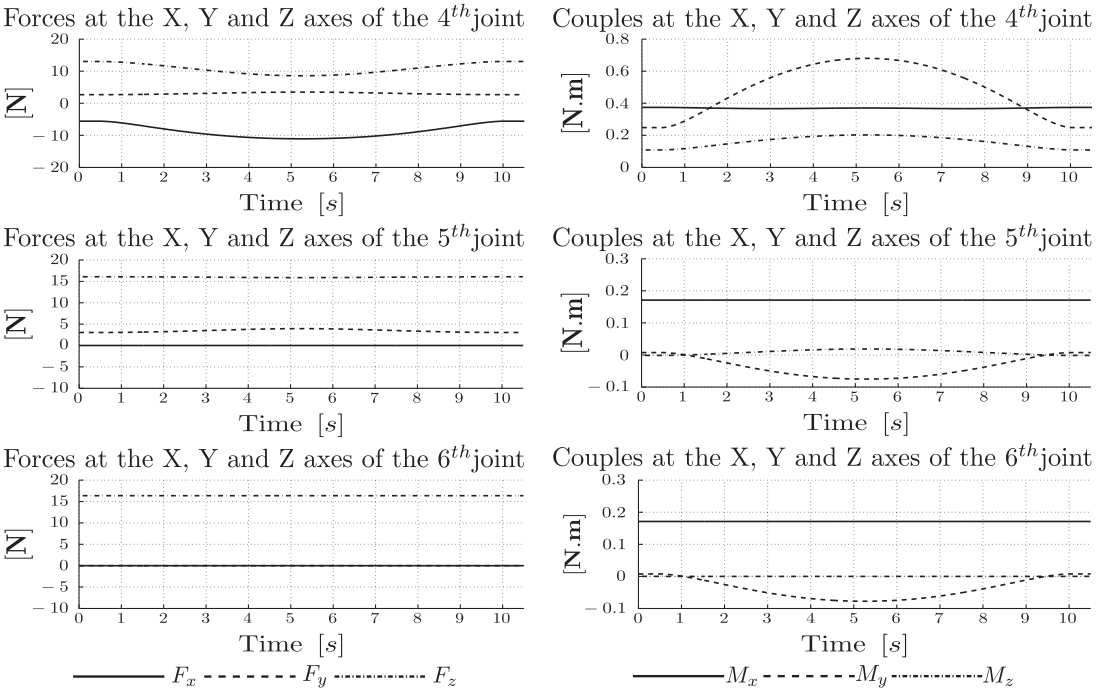


Fig. 9. Static action at the axes of the last three joints of the right leg during the simulation.

force of the CoM of each link. From this point of view, the weight of the links can be understood as perturbation forces as well.

Figures 8 and 9 depict forces and couples at the axes of the joints of the right leg. This estimated information is one of the main advantages of the kinetostatic model we propose. Considering that the rotation axes of the joints of the legs are Z, X, Y, Y, Y, and X, the required torques at the axis of each joint to make the postures of the *quasi*-static motion statically stable/feasible can be seen in Figures

https://doi.org/10.1017/S0263574717000595 Published online by Cambridge University Press

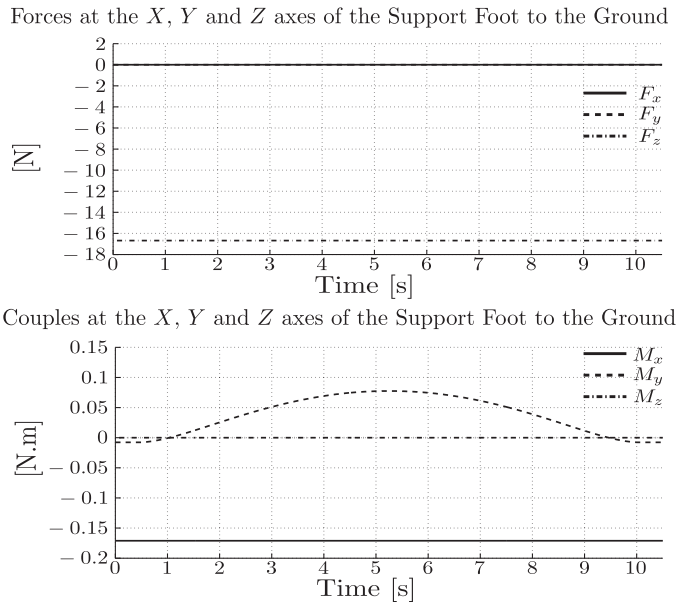


Fig. 10. Static action applied to the robot's supporting foot (right foot) to the ground (supporting surface) during the simulation.

8 and 9. Furthermore, in Figures 8 and 9, the magnitudes of the forces of constraint at all three axes of each joint and the transmitted couples generated are depicted.

The trajectory of the simulation's *quasi*-static motion was planned by establishing that the supporting foot was to be inertial on the ground during the entire motion, and it can be verified by the data presented in Fig. 10. It is possible to see that components F_x and F_y of the force $\boldsymbol{F}$ made by the supporting foot on the ground are null. It is also possible to observe that the component M_z of the couple generated between both the supporting foot and the ground is also null: there is no motion relative to the X and Y axes of the supporting foot, and the same foot does not have the tendency to rotate on its Z axis. On the other hand, the component F_z of the force $\boldsymbol{F}$ has a value in the same magnitude of the gravitational force of the total mass of the humanoid, which means that the robot is being supported by its supporting foot during the entire *quasi*-static motion of the simulation.

Furthermore, the component M_x of the couple $\boldsymbol{M}$ has constant value different from zero, which can be explained through the motion being a vertical displacement of the waist of the robot. This implies in no left-right displacement of the CoM of the robot. However, as the CoM moves forward and backward, the consequence is the non-zero and variable value of the component M_y of the couple $\boldsymbol{M}$: the couple that compensates the forward/backward motion of the CoM.

To demonstrate the capabilities of our kinetostatic model for HRs, let us comment on three other *quasi*-static motion simulations that were performed and whose results were uploaded as videos to YouTube. The first simulation (found at http://youtu.be/Vn55ZfL-yj4) aimed at moving the waist of the robot downwards and upwards while the robot was supported by both legs. Regarding the same simulation, another video (found at https://youtu.be/vJVOtLf1pjg) consisted of making the Bioloid HR execute said motion. The second simulation (found at https://youtu.be/DICKsM37Pb8) consisted of making the robot perform a gait, and it shows that the kinematic counterpart model is generic enough to perform any kind of motion without any change in the kinematic model. Finally, the third simulation (found at https://youtu.be/qOQLvm6C7ZQ) lasts 50*s* and, after the motion, the video depicts the numerical results obtained from the computation of the kinetostatic model.

5. Conclusions

In this paper, a modeling framework was proposed regarding the kinetostatic model of HRs based on screw theory, Assur's virtual chains, and Davies' method. Modeling this kind of robots using screw theory is a contribution in itself, since it provides a whole new set of tools that can be used in humanoid

https://doi.org/10.1017/S0263574717000595 Published online by Cambridge University Press

robotic systems, from the prototyping stage to kinematics and statics analysis, as well as the analysis of actual robots.

Differently from the major approaches that consider the "multi-model" methodology, this study presented a kinetostatic model that treats HRs as a parallel mechanism whose topological structure never changes. The proposed approach is able to represent both the kinematics and statics of said robots regardless of their posture, motion, and any other task to be performed by the robot.

The general approach of our kinetostatic model is sufficiently versatile to change the supporting condition, as developed in the essay, only by adding the contact condition of the left foot, which means that said foot would be, for example, above a ladder step. By applying minor changes to the model, it is not complex to adapt it to consider the single unknown contact condition at other links and, therefore, provide further contexts for analysis.

The static modeling approach presented in this paper provides a systematic methodology to compute the static acting forces and the couples at the three axes of each joint of the robot, and one unknown static contact condition that satisfies the static equilibrium. Indeed, by complying with the zero-moment point (ZMP) stability criterion, said estimated unknown static contact condition also makes both the posture and the quasi-static motion statically stable/feasible.

The resulting kinetostatic model has enough complexity to address any set of contacts between the robot limbs (feet and hands) and the environment. The solution of the static part of the proposed model is restricted to a single unknown contact constraint since two or more unknown contact conditions add redundancies to the system that we aim at addressing in future works when properly solved. Despite this current limitation, the proposed study presents a single, general, and systematic model that allows a general study of any HR (joints prototyping) in terms of its kinematics, statics, as well as its relationship with the environment. Said model can be directly used in designing phases of HRs such as type and dimensional synthesis. The evolution of the proposed methodology, which aims at both studying and analyzing HR dynamics, still contains problems to be solved, even though it already has potential for relevant future results.

Acknowledgment

The authors would like to thank UFSC and the Brazilian agencies CNPq and CAPES for the infrastructure and funding granted.

References

1. T. G. Ionescu, "Terminology for mechanisms and machine science," *Mecha. Mach. Theory* **38**(7–10), 819–825 (2003).
2. M. Khadiv, S. Moosavian, A. Ali and M. Sadedel, "Dynamics modeling of fully-actuated humanoids with general robot-environment interaction," *Proceedings of the International Conference on Robotics and Mechatronics*. IEEE 233–238 (2014).
3. S. A. Nugroho, A. S. Prihatmanto and A. S. Rohman, "Design and implementation of kinematics model and trajectory planning for nao humanoid robot in a tic-tac-toe board game," *Proceedings of the 4th International Conference on System Engineering and Technology*, IEEE **4**, 1–7 (2014).
4. M. Menad, Z. Derouiche, Z. A. Foitih and W. Nouibat, "Kinematic modeling of a humanoid robot with 18 dof in a virtual environment," *Proceedings of the International Conference on Innovative Computing Technology (InTECH)*. IEEE 424–429 (2013).
5. S. Moosavian, M. Alghooneh and A. Takhmar, "Modified transpose jacobian control of a biped robot," *Proceedings of the International Conference on Humanoid Robots*. IEEE 282–287 (2007).
6. H.-O. Lim, A. Ishii and A. Takanishi, "Emotion-based biped walking," *Robotica* **22**(5), 577–586 (2004).
7. X. Mu and Q. Wu, "A complete dynamic model of five-link bipedal walking," *Proceedings of the American Control Conference*, IEEE**6**, 4926–4931 (2003).
8. Q. Huang, K. Yokoi, S. Kajita, K. Kaneko, H. Arai, N. Koyachi and K. Tanie, "Planning walking patterns for a biped robot," *IEEE Trans. Robot. Autom.***17**(3), 280–289, (2001).
9. Y. Liu, P. M. Wensing, D. E. Orin and Y. F. Zheng, "Trajectory generation for dynamic walking in a humanoid over uneven terrain using a 3d-actuated dual-slip model," *Proceedings of the International Conference on Intelligent Robots and Systems*, IEEE, 374–380 (2015).
10. G. G. Muscolo, C. T. Recchiuto and R. Molfino, "Dynamic balance optimization in biped robots: Physical modeling, implementation and tests using an innovative formula," *Robotica* **33**(6), 1–17 (2015).
11. U. Nagarajan and K. Yamane, "Automatic task-specific model reduction for humanoid robots," *Proceedings of the International Conference on Intelligent Robots and Systems*, IEEE, 2578–2585 (2013).

https://doi.org/10.1017/S0263574717000595 Published online by Cambridge University Press

12. A. Akash, S. Chandra, A. Abha and G. Nandi, "Modeling a bipedal humanoid robot using inverted pendulum towards push recovery," *Proceedings of the International Conference on Communication, Information Computing Technology*, IEEE, 1–6 (2012).
13. X.-g. Ruan and Z.-q. Li, "A bipedal locomotion planning with double support phase based on linear inverted pendulum mode," *WRI Global Congr. Intell. Syst*., IEEE, **3**, 73–77 (2009).
14. K. Erbatur and U. Seven, "An inverted pendulum based approach to biped trajectory generation with swing leg dynamics," *Proceedings of the 7th International Conference on Humanoid Robots*, IEEE, (2007) pp. 216–221.
15. S. Kajita, O. Matsumoto and M. Saigo, "Real-time 3d walking pattern generation for a biped robot with telescopic legs," *Proceedings of the International Conference on Robotics and Automation*, IEEE, (2001) vol. **3**, pp. 2299–2306.
16. S. Kajita, F. Kanehiro, K. Kaneko, K. Yokoi and H. Hirukawa, "The 3d linear inverted pendulum mode: a simple modeling for a biped walking pattern generation," *Proceedings of the International Conference on Intelligent Robots and Systems*, IEEE (2001) vol. **1**, pp. 239–246.
17. S. Kajita, Y. Tomio and A. Kobayashi, "Dynamic walking control of a biped robot along a potential energy conserving orbit," *IEEE Trans. Robot. Autom*. **8**(4), 431–438 (1992).
18. Y. Umetani and K. Yoshida, "Resolved motion rate control of space manipulators with generalized jacobian matrix," *IEEE Trans. Robot. Autom.* **5**(3), 303–314 (1989).
19. S. Dubowsky and E. Papadopoulos, "The kinematics, dynamics, and control of free-flying and free-floating space robotic systems," *IEEE Trans. Robot. Autom.* **9**(5), 531–543 (1993).
20. E. Papadopoulos and S. Dubowsky, "On the nature of control algorithms for free-floating space manipulators," *IEEE Trans. Robot. Autom.* **7**(6), 750–758 (1991).
21. L. Sentis, "*Synthesis and Control of Whole-Body Behaviors in Humanoid Systems*," Ph.D. dissertation, (Stanford University, CA, USA, 2007).
22. O. Khatib, L. Sentis and J.-H. Park, "A unified framework for whole-body humanoid robot control with multiple constraints and contacts," In *European Robotics Symposium* (H. Bruyninckx, L. Preucil, M. Kulich, eds.) (Springer, Berlin, Heidelberg, 2008) pp. 303–312.
23. M. Mistry, J. Nakanishi, G. Cheng and S. Schaal, "Inverse kinematics with floating base and constraints for full body humanoid robot control," *Proceedings of the International Conference on Humanoid Robots*, IEEE (2008) pp. 22–27.
24. A. Mifsud, M. Benallegue and F. Lamiraux, "Estimation of contact forces and floating base kinematics of a humanoid robot using only inertial measurement units," *Proceedings of the International Conference on Intelligent Robots and Systems*, IEEE (2015) pp. 3374–3379.
25. A. Del Prete, N. Mansard, F. Nori, G. Metta and L. Natale, "Partial force control of constrained floating-base robots," *Proceedings of the International Conference on Intelligent Robots and Systems*, IEEE (2014) pp. 3227–3232.
26. Y. Guan, E. S. Neo, K. Yokoi and K. Tanie, "Stepping over obstacles with humanoid robots," *IEEE Trans. Robot.* **22**(5), 958–973 (2006).
27. K. Bouyarmane and A. Kheddar, "Multi-contact stances planning for multiple agents," *Proceedings of the International Conference on Robotics and Automation* (2011) pp. 5246–5253.
28. Y. Yokokohji, S. Nomoto, and T. Yoshikawa, "Static evaluation of humanoid robot postures constrained to the surrounding environment through their limbs," *Proceedings of the International Conference on Robotics and Automation*, IEEE, (2002), vol. **2**, pp. 1856–1863.
29. E. Yoshida, P. Blazevic and V. Hugel, "Pivoting manipulation of a large object: a study of application using humanoid platform," *Proceedings of the International Conference on Robotics and Automation* IEEE (Apr. 2005), pp. 1040–1045.
30. R. S. Ball, *A Treatise on the Theory of Screws*. (Cambridge University Press, Cambridge, UK, 1900), – reprinted in 1998.
31. K. H. Hunt, "Don't cross-thread the screw!" In *Symposium Commemorating The Legacy, Works and Life of Sir Robert Stawell Ball Upon the 100th Anniversary of A Treatise on The Theory of Screws* (Joseph Duffy, Hugh E. M. Hunt and Harvey Lipkin, eds.) (University of Cambridge, Trinity College. Cambridge: Cambridge University Press, 2000) pp. 1–37.
32. L.-W. Tsai, *Robot Analysis: The Mechanics of Serial and Parallel Manipulators*. (Wiley-Interscience, New York, 1999).
33. A. Campos, R. Guenther and D. Martins, "Differential kinematics of serial manipulators using virtual chains," *J. Braz. Soc. Mech. Sci. Eng.* **27**(4), 345–356 (2005).
34. C. Santos, R. Guenther, D. Martins and E. De Pieri, "Virtual kinematic chains to solve the underwater vehicle-manipulator systems redundancy," *J. Braz. Soc. Mech. Sci. Eng.* **28**, 354–361 (2006).
35. R. Guenther, H. Simas, D. da Cruz and D. Martins, "A new integration method for differential inverse kinematics of closed-chain robots," *Proceedings of the ABCM Symposium Series in Mechatronics*, ABCM **3**, 225–235 (2008).
36. G. S. Toscano, H. Simas and E. B. Castelan, "Trajectory generation for a spatial humanoid robots using assur virtual chains through screw theory," *Proceedings of the ABCM Symposium Series in Mechatronics*, ABCM **6**, (2014).
37. G. Mozzi, *Discorso Matematico Sopra il Rotamento Momentaneo Dei Corpi*. (Stamperia di Donato Campo, 1763).

https://doi.org/10.1017/S0263574717000595 Published online by Cambridge University Press

38. L. Poinsot, "Sur la composition des moments et la composition des aires," *J. de École Polytech.* **6**, 182–205 (1806).
39. O. O. Bottema and B. Roth, *Theoretical Kinematics*. (North-Holand Pub. Co., New York, 1979).
40. T. H. Davies, "Kirchhoff's circulation law applied to multi-loop kinematic chains," *Mech. Mach. Theory – Elsevier* **16**(3), 171–183 (1981).
41. H. Simas, R. Guenther, D. F. M. da Cruz and D. Martins, "A new method to solve robot inverse kinematics using assur's virtual chains," *Robotica – Cambridge University Press* **27**(07), 1017–1026 (2009).
42. J. K. Davidson and K. H. Hunt, *Robots and Screw Theory: Applications of Kinematics and Statics to Robotics*. (Oxford University Press, Oxford, UK, 2004).
43. J. Erthal, "Modelo cinemático pra análise de rolagem de veículos," Tese de doutorado, Universidade Federal de Santa Catarina (UFSC) - Departamento de Engenharia Mecânica (EMC) – Programa de Pós-graduação em Engenharia Mecânica (POSMEC), (Florianópolis – Brasil, 2010).
44. T. H. Davies, "Couplings, coupling network and their graphs," *Mech. Mach. Theory* **30**(7), 991–1000 (1995).
45. N. Christofides, *Graph Theory – An Algorithmic Approach*. (Academic Press Inc., New York, 1975).
46. M. Vukobratovic, B. Borovac and D. Surdilovic, "Zero-moment point–proper interpretation and new applications," *Proceedings of the International Conference on Humanoid Robots*, IEEE, **244** (2001).

https://doi.org/10.1017/S0263574717000595 Published online by Cambridge University Press